A&A 567, A22 (2014)
DOI: 10.1051/0004-6361/201423957

Astronomy & Astrophysics

Collisional excitation of O_2 by H_2: the validity of LTE models in interpreting O_2 observations

F. Lique[1], Y. Kalugina[1,2], S. Chefdeville[3], S. Y. T. van de Meerakker[4], M. Costes[3], and C. Naulin[3]

[1] LOMC – UMR 6294, CNRS-Université du Havre, 25 rue Philippe Lebon, BP 1123, 76063 Le Havre, France
e-mail: francois.lique@univ-lehavre.fr
[2] Department of Optics and Spectroscopy, Tomsk State University, 36 Lenin av., 634050 Tomsk, Russia
[3] Université de Bordeaux, Institut des Sciences Moléculaires, CNRS UMR 5255, 33405 Talence Cedex, France
[4] Radboud University Nijmegen, Institute for Molecules and Materials, Heijendaalseweg 135, 6525 AJ Nijmegen, The Netherlands

Received 7 April 2014 / Accepted 28 May 2014

ABSTRACT

Context. Oxygen molecules (O_2) are of particular interest because of their crucial role in astrochemisty. Modelling of O_2 molecular emission spectra from interstellar clouds requires the calculation of rate coefficients for excitation by collisions with the most abundant species.
Aims. Rotational excitation of $O_2(X^3\Sigma^-)$ by H_2 is investigated theoretically and experimentally and we check the validity of the local thermodynamic equilibrium (LTE) approach for interpreting O_2 observations.
Methods. Using a new ab initio potential energy surface, collisional excitation of O_2 is studied using a full close-coupling approach. The theoretical calculations are validated by comparison with crossed beam scattering experiments. We also performed calculations for the excitation of O_2 from a large velocity gradient (LVG) radiative transfer code using the new rate coefficients.
Results. State-to-state rate coefficients between the 27 lowest levels of O_2 were calculated for temperatures ranging from 5 K to 150 K. The critical densities of the O_2 lines are found to be at $\gtrsim 10^4$ cm^{-3} for temperatures higher than 50 K. This value is slightly larger than the one previously determined using previous He rate coefficients.
Conclusions. The new rate coefficients will help in interpreting O_2 emission lines observed where LTE conditions are not fully fulfilled and enable an accurate determination of the O_2 abundance in the interstellar medium.

Key words. molecular processes – molecular data – ISM: abundances – ISM: molecules

1. Introduction

Oxygen is the third most abundant element in the Universe after hydrogen and helium, which makes it very important in terms of understanding the formation and evolution of the chemistry in astronomical sources. Earlier gas-phase chemical models predicted O_2 to be a major reservoir of elemental oxygen in dense molecular clouds (Herbst & Klemperer 1973). Searches for interstellar O_2 have been one of the major goals for molecular astrophysics during the last decades. However, until recently, attempts to detect interstellar O_2 line emission with ground- and space-based observatories have failed (Combes & Wiklind 1995; Marechal et al. 1997; Pagani et al. 2003).

In 2007, Larsson et al. (2007) eventually reported the first observation of O_2 in the interstellar medium (ISM) from the satellite ODIN mission. Surprisingly, the O_2 abundance in the cores of molecular clouds was found to be ∼1000 times lower than predicted by the astrochemical models. The low O_2 abundance has since been confirmed by other O_2 observations (Goldsmith et al. 2011; Liseau et al. 2012; Yıldız et al. 2013).

Such a low abundance for the O_2 molecule pushed physical chemists and astrochemists to review the oxygen chemistry in dense molecular clouds (Lique et al. 2009). The low abundance of O_2 in dark clouds can now be explained by gas-grain chemical models that conclude that oxygen depletion is important (Hincelin et al. 2011).

Although low, the abundance of O_2 has still to be determined accurately. Since collisions compete with radiative processes in altering populations of molecular ro-vibrational levels, the estimation of molecular abundances in the ISM from spectral line data usually requires collisional rate coefficients with the most abundant interstellar species like He or H_2. Rate coefficients for O_2–He inelastic collisions were provided some time ago by Lique (2010). Goldsmith et al. (2011) used these rate coefficients to study the excitation of O_2 in cold molecular clouds. They concluded that O_2 abundance determination is possible assuming local thermodynamic equilibrium (LTE) (i.e. without using rate coefficients) because O_2 radiative rates are small and because the excitation of O_2 is dominated by collisions.

In the ISM, the main collisional partner is H_2 and it is well known that He and H_2 rate coefficients differ significantly, especially in the case of ortho-H_2 (Roueff & Lique 2013). It is then very important to also provide collisional data for the O_2–H_2 systems.

In this paper, we present a new study of the collisional excitation of O_2 by H_2 and we compare the theoretical results with experimental ones obtained from crossed-beam scattering experiments. Using the new data, we check the validity of the LTE approach for interpreting O_2 observations.

2. Methodology of calculations

2.1. Potential energy surface (PES)

The PES used in this work was described in detail in Kalugina et al. (2012, hereafter Paper I). The PES was calculated in the supermolecular approach with a partially spin-restricted coupled cluster with single, double, and perturbative triple excitations [RCCSD(T)] (Knowles et al. 1993, 2000). The collision partners were considered to be rigid [r_{O-O} = 2.297 bohr and r_{H-H} = 1.449 bohr]. The four atoms were described by augmented correlation-consistent quadruple zeta (aug-cc-pVQZ) basis set of Dunning (1989) augmented with bond functions. Details of computations, analytical representation, and plots of the PES are given in Paper I. For the scattering calculations, we used the original PES of Paper I and not the scaled one of Chefdeville et al. (2013).

2.2. Scattering calculations

As noticed in Paper I and confirmed by the experiments of Chefdeville et al. (2013), the rotation of H_2 has almost no influence on the magnitude of O_2–H_2 integral cross sections (ICS). Thus, we performed calculations only for the $j = 0$ level of H_2 (i.e. the PES was averaged over both orientation θ' and dihedral ϕ angles describing the H_2 geometry) and considered that our results are valid for both para- and ortho-H_2. Collisions with $H_2(j = 0)$ are equivalent to collisions with a structureless atom. Then, the scattering problem is equivalent to atom-diatom inelastic collisions.

In the $O_2(^3\Sigma^-)$ electronic ground state, the rotational levels are split by spin-rotation coupling. In the intermediate coupling scheme, the rotational wave function of O_2 can be written for $j \geq 1$ as (Lique et al. 2005)

$$\begin{aligned} |F_1 jm\rangle &= \cos\alpha|N = j-1, S\ jm\rangle + \sin\alpha|N = j+1, S\ jm\rangle \\ |F_2 jm\rangle &= |N = j, S\ jm\rangle \\ |F_3 jm\rangle &= -\sin\alpha|N = j-1, S\ jm\rangle + \cos\alpha|N = j+1, S\ jm\rangle, \end{aligned} \quad (1)$$

where $|N, S\ jm\rangle$ denotes pure Hund's case (b) basis functions and the mixing angle α is obtained by diagonalisation of the molecular Hamiltonian. In this relation corresponding to Hund's case (b), the total molecular angular momentum j is defined by:

$$j = N + S, \quad (2)$$

where N and S are the nuclear rotational and the electronic spin angular momenta. The rotational energy levels of the O_2 molecule were computed with the use of the experimental spectroscopic constants of Endo & Mizushima (1982).

All calculations were carried out with the exact energy levels including the fine structure interaction. However, in the present paper, we will use the usual astrophysical level labelling N_j where $N = j - 1$, $N = j$, and $N = j + 1$ correspond to the F_1, F_2, and F_3 levels as defined in Eq. (1). The quantal coupled equations were solved in the intermediate coupling scheme using the MOLSCAT code (Hutson & Green 1994) modified to take into account the fine structure of the energy levels. We used a fine collisional energy grid for the calculations so that the resonances (shape and Feshbach) that appear in the ICS at low and intermediate energies were well represented.

By averaging over a Maxwellian distribution of collision velocities, we can use the calculated ICS to obtain thermal rate coefficients for (de-)excitation transitions between O_2 levels

$$k_{\alpha\to\beta}(T) = \left(\frac{8}{\pi\mu k_B^3 T^3}\right)^{\frac{1}{2}} \int_0^\infty \sigma_{\alpha\to\beta}\, E_k\, e^{-\frac{E_k}{k_B T}}\, dE_k, \quad (3)$$

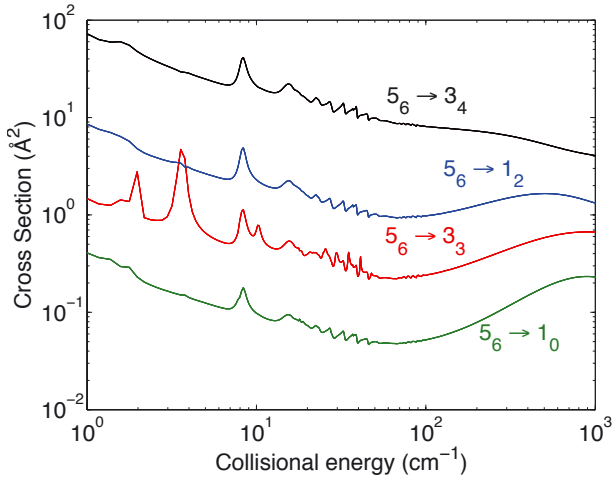

Fig. 1. Collisional excitation ICS of O_2 by H_2 out of the $N_j = 5_6$ state.

where $\sigma_{\alpha\to\beta}$ is the cross section from initial level α (i.e. N_j) to final level β (i.e. $N'_{j'}$), μ is the reduced mass of the system and k_B is the Boltzmann constant.

In order to ensure convergence of the inelastic ICS, it was necessary to include in the calculations several energetically inaccessible (closed) levels. At the largest energies considered in this work, the O_2 rotational basis was extended to $N = 29$ to ensure convergence of the rotational ICS of O_2.

3. Results

3.1. Cross sections

We have obtained the (de-)excitation ICS between the first 27 fine structure levels of O_2 by H_2. Figure 1 presents the typical kinetic energy variation of the ICS for de-excitation transitions from the $N_j = 5_6$ level of O_2. As expected, the de-excitation ICS decrease with increasing energy. Noticeable resonances appear at low collisional energies. This is related to the presence of an attractive potential well, which allows for O_2–H_2 bound and quasi-bound states to be formed before the complex dissociates (Smith et al. 1979; Christoffel & Bowman 1983).

The quality of the theoretical results strongly depends on the accuracy of the PES employed for the quantum scattering calculations, especially at very low energy and for low O_2 quantum numbers where the ICS can be significantly dominated by resonances. The energy position, width and magnitude of the resonances are so dependent on the calculated potential well that their experimental observation offers a stringent test for the theory. We already obtained a strong positive sign in previous combined theoretical and experimental work on the ICS of the $1_0 \to 1_1$ transition with complete resolution of the partial-wave resonances (Chefdeville et al. 2013). In this work, we extend the study to the $1_2 \to 3_2$ transition.

Using the same apparatus as the one described in Chefdeville et al. (2013), we measured the ICS corresponding to the $1_2 \to 3_2$ transitions by probing the collision induced population in the 3_2 level as a function of the collision energy using the $2+1(^3\Sigma_1^-,\ v = 2 \leftarrow {}^3\Sigma_g^-, v = 0)\ Q_{23}(2)$ resonance-enhanced multiphoton ionisation transition at 88.874 cm^{-1} (Yokelson et al. 1992). The experiments were performed with normal-H_2; they can nevertheless be directly compared with the theoretical results since the O_2–H_2 ICS have been proven not to depend on the

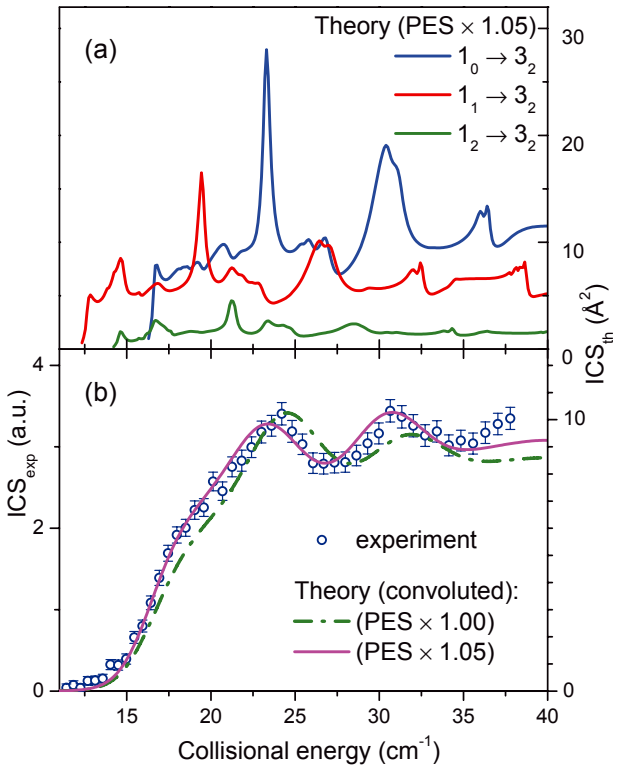

Fig. 2. Collisional energy dependence of the integral cross sections for O_2 excitation $N_j = 1_0 \rightarrow N'_{j'} = 3_2$. **a)** Theoretical ICS calculated with modified PES; **b)** theoretical ICS convoluted with the experimental collision energy spread calculated with the original PES (dashed line) and the modified PES (solid line); experimental data (open circles), obtained when crossing a beam of normal-H_2 from a first pulsed nozzle at ≃45 K propagating at velocity $v_1 = 951$ ms^{-1} with a beam of 0.5% O_2 in Ne from a second pulsed nozzle at 300 K propagating at $v_2 = 803$ ms^{-1}; crossing angle χ was varied from 22.5° to 45°, resulting in a collision energy $E_k = \frac{1}{2}\mu(v_1^2 + v_2^2 - 2v_1v_2\cos\chi)$ where μ stands for the reduced mass of the collision partners.

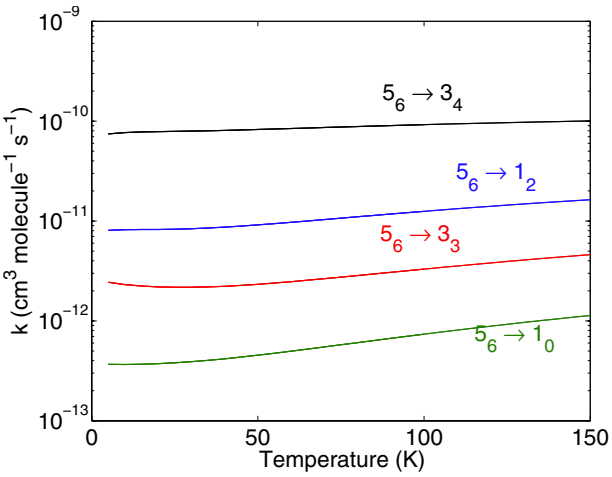

Fig. 3. O_2–H_2 rate coefficients out of the $N_j = 5_6$ state.

rotational levels of H_2. The initial residual population in 3_2 level was offset by shot-to-shot background subtraction when triggering the probe laser and the O_2 beam at 10 Hz with the H_2 beam at 5 Hz. The ICS were recovered from the measured intensities using the procedure described in the Supplementary Materials of Chefdeville et al. (2013).

The ICS obtained for O_2–H_2 collisions are displayed in Fig. 2. The theoretical results obtained with a slightly modified PES (the original PES scaled by a factor of 1.05; see Chefdeville et al. 2013) for the three possible transitions from the $N = 1$ state ($1_{j=0-2} \rightarrow 3_2$) are given in the upper panel (Fig. 2a). The experimental data obtained between $E_k = 11.4$ cm^{-1} and 37.8 cm^{-1} are displayed in the lower panel (Fig. 2b) along with the theoretical ICS convoluted with the experimental collision energy spread to allow for comparison with the experimental values. Excitation of any $1_{j=0-2}$ state can contribute to the signal. However, the observed signal is probably due mainly to the 1_0 state for the following reasons: (i) the rotational temperature within the molecular beam for CO (Chefdeville et al. 2012) and O_2 (Chefdeville et al. 2013) beams was proven to be below 1 K; a similar behaviour is then expected for the O_2 source in the present work, resulting in relative populations ($P(0) \simeq 0.8$, $P(2) \simeq 0.2$ and $P(1) \leq 0.01$); (ii) the calculated cross section for excitation of the $N_j = 1_1$ state ($\Delta j = \Delta N - 1$) is only slightly less intense than for the $N_j = 1_0$ state ($\Delta j = \Delta N$); a significant population of the $N_j = 1_1$ level would result in a significant signal below the $1_0 \rightarrow 3_2$ threshold at 16.3 cm^{-1}, which is not observed; and (iii) the calculated cross section for excitation from the 1_2 level is much weaker ($\Delta j = \Delta N - 2$); a 20% population results in a small contribution. The theoretical data displayed in Fig. 2b are the sum of the contributions of excitation from the 1_0, 1_2, and 1_1 states, weighted to their relative populations at 1 K, and convoluted to experimental energy resolution.

The agreement between experimental values and present theory is good. The agreement becomes almost perfect as for the $1_0 \rightarrow 1_1$ transition when using the slightly modified PES. However, this modified PES, tailored for very low collisional energies, can hardly be used for the determination of rate coefficients for temperatures above 30–50 K. This PES accurately describes the bound state energies but the scaling factor of 1.05 leads to an overestimation of the interaction energies in the repulsive wall. For the original PES, the overall good agreement again confirms the accuracy of the calculated PES and of the theoretical approach. We found that rate coefficients obtained from both the original and the modified PES differ by less than 10% at 10K. It suggests that the rate coefficients obtained here are accurate enough to allow improved astrophysical modelling.

3.2. Rate coefficients

By performing a thermal average of the collision energy dependent ICS, we have obtained rate coefficients between the first 27 fine structure O_2 levels for temperatures up to 150 K. This complete set of (de-)excitation rate coefficients is available on-line from the LAMDA (Schöier et al. 2005) and BASECOL (Dubernet et al. 2013) websites. The thermal dependence of the state-to-state O_2–H_2 rate coefficients is illustrated in Fig. 3 for transitions out of the $N_j = 5_6$ level.

A strong propensity rule exists for $\Delta j = \Delta N$ transitions. A propensity rule of this kind was predicted theoretically (Alexander & Dagdigian 1983) and is general for molecules in the $^3\Sigma^-$ electronic state. It was also observed previously for the $O_2(X^3\Sigma^-)$–He (Lique 2010), $SO(X^3\Sigma^-)$–H_2 (Lique et al. 2007) or $NH(X^3\Sigma^-)$–He (Toboła et al. 2011) collisions.

Collisions with He are often used to model collisions with H_2. It is generally assumed that rate coefficients with H_2 should be larger than He rate coefficients; a scaling factor of 1.4 being often used (Schöier et al. 2005). In Table 1, we show,

Table 1. Comparison between O_2–He and present O_2–H_2 rate coefficients.

	10 K		50 K		150 K	
$N_j \rightarrow N'_{j'}$	He	H_2	He	H_2	He	H_2
$1_1 \rightarrow 1_0$	0.14	0.76	0.04	0.17	0.01	0.04
$3_3 \rightarrow 1_1$	1.75	3.76	2.35	3.99	3.06	5.29
$3_3 \rightarrow 1_2$	1.08	1.95	1.38	1.96	1.90	2.65
$3_4 \rightarrow 1_0$	0.18	0.28	0.21	0.27	0.37	0.51
$3_4 \rightarrow 1_2$	2.56	5.76	3.37	5.95	4.28	7.72
$5_4 \rightarrow 1_0$	0.21	0.28	0.27	0.31	0.44	0.53
$5_4 \rightarrow 1_2$	0.19	0.24	0.28	0.28	0.61	0.60
$5_4 \rightarrow 3_2$	3.27	6.39	3.89	6.84	4.64	8.14
$9_{10} \rightarrow 5_6$	0.87	1.58	1.29	1.81	2.21	2.84
$9_{10} \rightarrow 7_7$	0.06	0.09	0.10	0.10	0.22	0.19

Notes. The rate coefficients are in units of 10^{-11} cm^3 s^{-1}.

on a small sample, a comparison of our rotational O_2–H_2 rate coefficients versus the O_2–He ones of Lique (2010).

As one can see, differences exist between the two sets of data. Globally, the H_2 results are larger by a factor of $\simeq$2 than the He ones at low temperature and for transitions between the first rotational states. The ratio can even be larger (see e.g. the $1_1 \rightarrow 1_0$ transition). However, for transitions between higher energy levels and for temperature above 50 K, He rate coefficients can be equal to or larger than the H_2 rate coefficients. Therefore, using He rate coefficients scaled by a factor of 1.4 results in an overestimation of the collisional process in modelling of O_2 emission.

4. Discussion and astrophysical applications

We have presented quantum mechanical calculations of rate coefficients for the collisional excitation of O_2 by H_2 molecules. The accuracy of the theoretical calculations has been checked by comparing theoretical and experimental ICS. The rotationally inelastic energy transfer in O_2 is more efficient with H_2 molecules than with He atoms at low temperature, but is similar at high temperatures and for high rotational states.

As a first application and in order to test the impact of the new rate coefficients, we have performed radiative transfer calculations for typical physical conditions from where O_2 emission is detected. Non-local thermodynamic equilibrium (non-LTE) calculations were performed with the RADEX code (van der Tak et al. 2007) using the large velocity gradient (LVG) approximation for an expanding sphere. Both collisional and radiative processes are taken into account.

We focus on the calculation of the excitation temperature determined for O_2 transitions that have been already observed. Figure 4 shows some results of our calculations for a column density of O_2 fixed at 10^{15} cm^{-2}.

At very low volume densities, the excitation temperature of four lines tends to be equal to the adopted value of the background radiation field (2.7 K). This parameter rises to higher values as collisional excitation becomes more important. At volume densities above a critical value, the excitation temperature approaches the kinetic temperature, at which point the LTE approximation may be used. At low temperatures (10 K) the critical density lies at $\approx 10^3$ cm^{-3}, while for higher temperatures, the critical density can be up to $2-3 \times 10^4$ cm^{-3} for transitions between highly excited states. This conclusion is in reasonable agreement

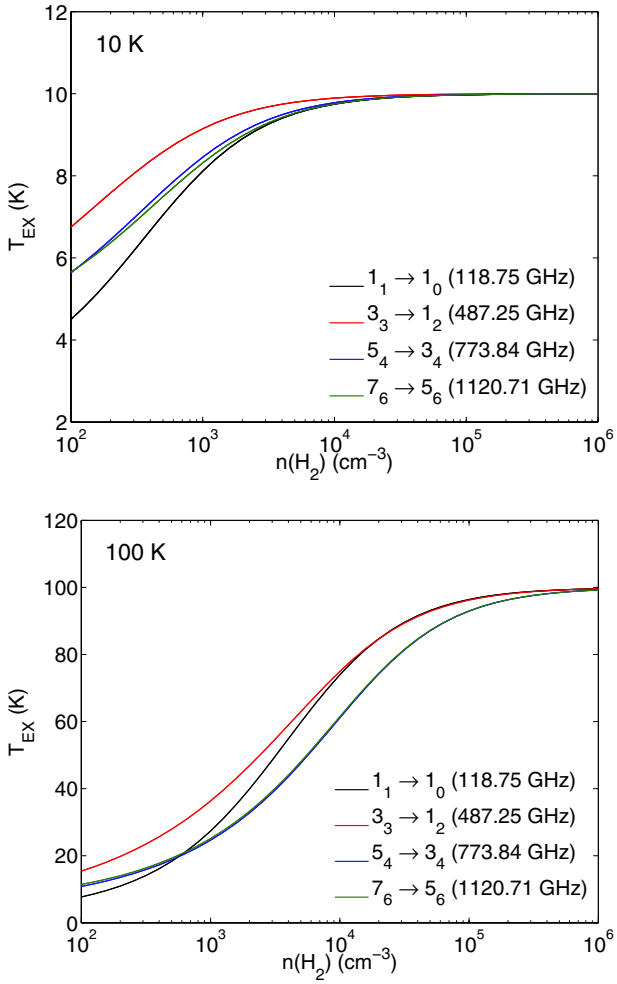

Fig. 4. Excitation temperature for the $1_1 \rightarrow 1_0$, $3_3 \rightarrow 1_2$, $5_4 \rightarrow 3_4$ and $7_6 \rightarrow 5_6$ lines of O_2, as a function of volume density for $T = 10$ and 100 K. The column density of O_2 is 10^{15} cm^{-2}.

with the one found by Goldsmith et al. (2011) although we found critical densities a bit larger than in their study. This can certainly be explained by the magnitude of H_2 rate coefficients between high energy levels of O_2 that is smaller than the corresponding He ones (scaled by a factor of 1.4) used by Goldsmith et al. (2011).

We also vary the column density of O_2 (from 10^{14} to 10^{16} cm^{-2}) and we have also found although not shown here that the column density has almost no impact on the magnitude of the excitation temperature. This can certainly be explained by the fact that the O_2 lines are optically thin.

To conclude, at typical physical conditions of molecular clouds where O_2 is observed ($n(H_2) > 3 \times 10^4$ cm^{-3}, $T = 10-100$ K), O_2 lines are mainly thermalised. However, if O_2 can survive in slightly lower density and/or higher temperature molecular clouds, non-LTE analysis will be required in order to enable an accurate determination of O_2 abundance.

Acknowledgements. This research was supported by the CNRS national program "Physique et Chimie du Milieu Interstellaire". We also thank the CPER Haute-Normandie/CNRT/Énergie, Électronique, Matériaux. This work extends the objectives of ANR-12-BS05-0011-02 contract with the Agence Nationale de la Recherche for which financial support is gratefully acknowledged. Scattering calculations were carried out using HPC resources of SKIF Cyberia (Tomsk State University). We thank Alexandre Faure for helpful discussion.

References

Alexander, M. H., & Dagdigian, P. J. 1983, J. Chem. Phys., 79, 302
Chefdeville, S., Stoecklin, T., Bergeat, A., et al. 2012, Phys. Rev. Lett., 109, 023201
Chefdeville, S., Kalugina, Y., van de Meerakker, S. Y. T., et al. 2013, Science, 341, 1094
Christoffel, K. M., & Bowman, J. M. 1983, J. Chem. Phys., 78, 3952
Combes, F., & Wiklind, T. 1995, A&A, 303, L61
Dubernet, M.-L., Alexander, M. H., Ba, Y. A., et al. 2013, A&A, 553, A50
Dunning, T. H. 1989, J. Chem. Phys., 90, 1007
Endo, Y., & Mizushima, M. 1982, Japanese J. Appl. Phys., 21, L379
Goldsmith, P. F., Liseau, R., Bell, T. A., et al. 2011, ApJ, 737, 96
Herbst, E., & Klemperer, W. 1973, ApJ, 185, 505
Hincelin, U., Wakelam, V., Hersant, F., et al. 2011, A&A, 530, A61
Hutson, J. M., & Green, S. 1994, MOLSCAT computer code, version 14, distributed by Collaborative Computational Project No. 6 of the Engineering and Physical Sciences Research Council (UK)
Kalugina, Y., Denis Alpizar, O., Stoecklin, T., & Lique, F. 2012, Phys. Chem. Chem. Phys., 14, 16458 (Paper I)
Knowles, P. J., Hampel, C., & Werner, H.-J. 1993, J. Chem. Phys., 99, 5219
Knowles, P. J., Hampel, C., & Werner, H.-J. 2000, J. Chem. Phys., 112, 3106
Larsson, B., Liseau, R., Pagani, L., et al. 2007, A&A, 466, 999
Lique, F. 2010, J. Chem. Phys., 132, 044311
Lique, F., Spielfiedel, A., Dubernet, M. L., & Feautrier, N. 2005, J. Chem. Phys., 123, 134316
Lique, F., Senent, M., Spielfiedel, A., & Feautrier, N. 2007, J. Chem. Phys., 126, 164312
Lique, F., Jorfi, M., Honvault, P., et al. 2009, J. Chem. Phys., 131, 221104
Liseau, R., Goldsmith, P. F., Larsson, B., et al. 2012, A&A, 541, A73
Marechal, P., Pagani, L., Langer, W. D., & Castets, A. 1997, A&A, 318, 252
Pagani, L., Olofsson, A. O. H., Bergman, P., et al. 2003, A&A, 402, L77
Roueff, E., & Lique, F. 2013, Chem. Rev., 113, 8906
Schöier, F. L., van der Tak, F. F. S., van Dishoeck, E. F., & Black, J. H. 2005, A&A, 432, 369
Smith, L. N., Malik, D. J., & Secrest, D. 1979, J. Chem. Phys., 71, 4502
Toboła, R., Dumouchel, F., Kłos, J., & Lique, F. 2011, J. Chem. Phys., 134, 024305
van der Tak, F. F. S., Black, J. H., Schöier, F. L., Jansen, D. J., & van Dishoeck, E. F. 2007, A&A, 468, 627
Yıldız, U. A., Acharyya, K., Goldsmith, P. F., et al. 2013, A&A, 558, A58
Yokelson, R. J., Lipert, R. J., & Chupka, W. A. 1992, J. Chem. Phys., 97, 6153